(2)

OFFICE OF NAVAL RESEARCH

GRANT NO. N00014-91-J-1447
R&T CODE 414044

Technical Report No. 22

DECOMPOSITION STUDIES OF TRIISOPROPYLANTIMONY AND TRIALLYLANTIMONY

by

S.H. LI, C.A. LARSEN, G.B. STRINGFELLOW, and R.W. GEDRIDGE, JR.

Prepared for Publication

in the

Journal of Electronic Materials

University of Utah
Dept. of Materials Science & Engineering
Salt Lake City, UT 84112

May 22, 1992

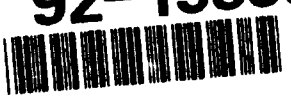

Decomposition Studies of Triisopropylantimony and Triallylantimony

S. H. Li, C. A. Larsen*, and G. B. Stringfellow,
Department of Materials Science and Engineering,
University of Utah, Salt Lake City, UT 84112;
R. W. Gedridge, Jr.,
Chemistry Division, Research Department,
Naval Weapons Center, China Lake, CA 93555

Abstract

The pyrolysis of triisopropylantimony ($(C_3H_7)_3Sb$) and triallylantimony ($(C_3H_5)_3Sb$) has been investigated mass-spectrometrically in He and D_2 using an SiO_2 flow tube reactor at atmospheric pressure. Both temperature and time dependencies of percent decomposition were studied and the reaction products were analyzed. The overall decomposition processes for both compounds were found to be homogeneous and first order. $(C_3H_7)_3Sb$ pyrolyzes at 250-350°C with no effect of the ambient gas. However, C_3H_6, C_3H_8, and C_6H_{14} (2,3-dimethylbutane) were produced in He whereas C_3H_7D appeared in D_2. The pyrolysis is believed to begin via bond cleavage to generate the free C_3H_7 radicals that, in turn, recombine and disproportionate. Isopropyl radicals react slowly with D_2, producing the C_3H_7D detected. For $(C_3H_5)_3Sb$, the pyrolysis takes place at 100-160°C. The only major product is C_6H_{10} (1,5-hexadiene). Both the pyrolysis rate and products were independent of the ambient. Two possible mechanisms, homolysis and reductive coupling, are discussed. Assuming that homolysis is the rate-limiting step for the pyrolysis of both $(C_3H_7)_3Sb$ and $(C_3H_5)_3Sb$, bond strengths of 30.8 and 21.6 kcal/mole for C_3H_7—Sb and C_3H_5—Sb were determined from the experimental data. When either $(C_3H_7)_3Sb$ or $(C_3H_5)_3Sb$ was mixed with trimethylindium, a non-volatile, liquid material, probably an adduct, was formed.

Keywords: triisopropylantimony, triallylantimony, pyrolysis, OMVPE.

* Current Address: Dept. Electronic Materials Engineering, Research School of Physical Sciences, Australian National University, GPO Box 4, ACT 2601

1. Introduction

InSb and related alloys have direct bandgaps and extremely high intrinsic electron mobilities. This makes these materials attractive for both electronic and long-wavelength photonic devices. Quantum well/superlattice structures can be prepared using the organometallic vapor-phase epitaxy (OMVPE) technique [1]. However, these materials must be produced at relatively low temperatures. The melting point of InSb is only 524°C. At growth temperatures this low, the cost for a run may be unacceptably high because the precursors, especially the commonly-used Sb precursor trimethylantimony ($(CH_3)_3Sb$), cannot efficiently decompose [2-4]. For example, InAsSbBi quaternary crystals need to be grown at approximetely 300°C [5] where the $(CH_3)_3Sb$ decomposition percentage is less than 5% [2]. Therefore, more than 95% of the expensive source is wasted.

Efforts have recently been made to develop alternative, low-decomposition-temperature Sb precursors. Triisopropylantimony ($(C_3H_7)_3Sb$) has been successfully used to grow InSb at temperatures as low as 300°C [6,7]. Such growth temperatures are difficult using $(CH_3)_3Sb$ because of the slow pyrolysis rate. The capability for $(C_3H_7)_3Sb$ to grow materials at lower temperatures than those for $(CH_3)_3Sb$ is a direct result of the lower bond strength of C_3H_7—Sb relative to CH_3—Sb. The C_3H_7—H bond strength is 95.1 kcal/mole, significantly lower than that for CH_3—H, 105.1 kcal/mole [8]. This bond strength/growth temperature relationship suggests that triallylantimony ($(C_3H_5)_3Sb$) may allow even lower growth temperatures: The C_3H_5—H bond strength is only 86.3 kcal/mole [8].

In this work, the pyrolysis reactions for $(C_3H_7)_3Sb$ and $(C_3H_5)_3Sb$ have been investigated mass-spectrometrically in He and D_2. The pyrolysis temperatures were measured, the products analyzed, and the reaction orders examined. The purpose of using D_2 instead of H_2 in this study is to label the pyrolysis products without appreciably altering the chemistry. This can resolve the role of H_2 in OMVPE growth. For some experiments, the reactor was packed to give a high surface area to determine whether the reaction is homogeneous or heterogeneous. A radical scavenger (1,4-cyclohexadiene, C_6H_8) was also added to probe the role of free radicals in the pyrolysis process. Finally, each of the Sb precursors was mixed with trimethylindium ($(CH_3)_3In$) to study the In/Sb precursor interactions. The results of these studies provide important insights into the decomposition mechanisms. The information is useful for the design of Sb precursors and for the development of a low temperature OMVPE growth process for Sb-containing materials.

2. Experimental

The experiments were conducted in an isothermal, flow-tube, SiO_2 reactor at atmospheric pressure (635 Torr in Salt Lake City). The diameter and the length of the reactor are 0.4 and 41.5 cm, respectively. The total gas flow rate was 40 sccm for the temperature dependence studies. However, for the time dependence studies, it was varied between 20-100 sccm. The effluent gas was sampled into a time-of-flight mass spectrometer via an adjustable leak. A schematic diagram of the apparatus has been pubished previously [9].

The synthesis of $(C_3H_7)_3Sb$ and $(C_3H_5)_3Sb$ was accomplished using the Schlenk techniques [10]. $(C_3H_7)_3Sb$ was prepared by the reaction of $SbCl_3$ with C_3H_7MgCl in C_4H_8O [11]. $(C_3H_5)_3Sb$ was produced in a similar manner [12]. Colorless liquids were collected after filtration and precipitation. Subsequently, the liquids were purified by fractional vacuum distillation. Characterization was carried out by the ^1H and ^{13}C NMR spectroscopy. The vapor pressures at various temperatures were determined using a Hg manometer.

For the pyrolysis experiments, an ionization energy of 70 eV was used in the mass spectrometer. Mass spectra for $(C_3H_7)_3Sb$ and $(C_3H_5)_3Sb$ at room temperature were obtained first. Spectra for other reactants and products were acquired from the literature [13]. The *ionization cross-sectional* area for each molecule was assumed to be the sum of those of its constitutent atoms [14]. These procedures enabled the quantitative analysis of the percent decomposition and the concentrations of the reaction products. The mass spectrometer detectability limit was approximately 0.02%.

3. Results

3.1 Vapor Pressures and Mass Spectra

The vapor pressures for $(C_3H_7)_3Sb$ and $(C_3H_5)_3Sb$ at different temperatures are listed in table 1. While they are low as compared to those for $(CH_3)_3Sb$ and trivinylantimony ($(C_2H_3)_3Sb$) [15], their room temperature vapor pressures are sufficient for OMVPE growth [7,16].

The relative intensities of the major mass-spectral peaks for $(C_3H_7)_3Sb$ and $(C_3H_5)_3Sb$ (0.05% in He for both) are shown in table

2. The principle peaks correspond to the $C_3H_7^+$ and $C_3H_5^+$ species for $(C_3H_7)_3Sb$ and $(C_3H_5)_3Sb$, respectively. The parent peak of $(C_3H_7)_3Sb$ (molecular weight: 251) was monitored, whereas that for $(C_3H_5)_3Sb$ (molecular weight: 245) is undetectable, probably due to the very low bond strength of C_3H_5—Sb.

3.2. Effect of Ambient and Surface Area

Using the peaks at m/e=251 for $(C_3H_7)_3Sb$ and m/e=204 for $(C_3H_5)_3Sb$, the relative reactant concentrations at each temperature were determined. The temperature dependence of the percent decomposition under various conditions is plotted in Fig.1, for $(C_3H_7)_3Sb$ and $(C_3H_5)_3Sb$, individually. The results for pyrolysis of $(CH_3)_3Sb$ and $(C_2H_3)_3Sb$ in He are also shown for comparison [2,17]. A change of the ambient from He to D_2 had no effect on the decomposition temperatures of either $(C_3H_7)_3Sb$ or $(C_3H_5)_3Sb$. This indicates that either intramolecular reactions dominate or that free radicals produced do not react rapidly with D_2. These results are similar to those reported previously for $(C_2H_3)_3Sb$ [17]; they are different from those for $(CH_3)_3Sb$. The presence of D_2 has no apparent effect on the decomposition of $(C_2H_3)_3Sb$ [17], but D_2 reduces the $(CH_3)_3Sb$ decomposition temperature by more than 50° [2].

Increasing the surface area by a factor of 24 (the reactor was packed with SiO_2 chips with surface area determined by measuring the chip size) increases the decomposition rate slightly for $(C_3H_7)_3Sb$ and not at all for $(C_3H_5)_3Sb$. The $(C_3H_7)_3Sb$ decomposition temperature was reduced by approximately 25°. Since a completely-heterogeneous reaction rate is proportional to the surface area, the

decomposition temperature for a 24-fold surface area can be calculated. The result is that the temperature should be decreased by 100° if an activation energy of 20 kcal/mole is assumed [18]. The pyrolysis processes for both precursors are believed to be mainly homogeneous. Homogeneous pyrolysis mechanisms have been also reported for $(CH_3)_3Sb$ and $(C_2H_3)_3Sb$ [2,17].

3.3. Pyrolysis Products

The pyrolysis products for $(C_3H_7)_3Sb$ in He and D_2 are given in Figs. 2a and 2b. The main products in He are C_3H_6, C_3H_8, and C_6H_{14} (2,3-dimethylbutane). C_3H_6, C_3H_8, C_6H_{14}, and C_3H_7D were the products in D_2. Although the effect of D_2 on the decomposition rate was slight, the deuterated product C_3H_7D was found in D_2. The same characteristics have been observed for triethylarsine ($(C_2H_5)_3As$): D_2 has no effect on the decomposition temperature, but C_2H_5D was produced [19]. These data suggest that the free C_3H_7 radicals produced from $(C_3H_7)_3Sb$ homolysis react slowly with D_2 to produce C_3H_7D. The majority of the free C_3H_7 radicals recombine and disproportionate to form the C_3H_6, C_3H_8, and C_6H_{14} observed. D atoms produced from the C_3H_7/D_2 reaction play no important role in accelerating the $(C_3H_7)_3Sb$ decomposition.

The concentrations of the products C_3H_6 and C_3H_8 from disproportionation reaction are expected to be in a 1:1 ratio. However, more C_3H_6 than C_3H_8 was observed in both He and D_2, as shown in Figs. 2a and 2b. This indicates the possibility of a parallel β-hydrogen elimination reaction. The β-hydrogen elimination reaction for $(C_3H_7)_3Sb$ may produce C_3H_6 and $(C_3H_7)_2SbH$. The latter could not be detected in this study because its concentration was small and

the mass spectral peaks overlapped those of $(C_3H_7)_3Sb$. Competing homolysis and β-hydrogen elimination reactions have been proposed for the pyrolysis of the related compound diisopropyltelluride ($(C_3H_7)_2Te$) [20].

Figs. 3a and 3b display the pyrolysis products for $(C_3H_5)_3Sb$ in He and D_2. The only detectable species was C_6H_{10} (1,5-hexadiene) for both ambient gases. Obviously a C_6H_{10} molecule can be formed by recombination of two C_3H_5 radicals. But, whether free radicals were existent during pyrolysis is unknown. C_3H_5 radicals may be too stable to react with D_2, leading to the observation of no deuterated products.

In addition to the gaseous products discussed above, solid Sb deposits were observed in the reactor for both precursors. This combined with the observation of the insignificant effect of the surface area on the decomposition rates indicates that the Sb surface does not significantly catalyze the pyrolysis for either $(C_3H_7)_3Sb$ or $(C_3H_5)_3Sb$.

3.4. Reaction Order

The reaction order has been studied for the pyrolysis of both $(C_3H_7)_3Sb$ and $(C_3H_5)_3Sb$. The time allowed for pyrolysis is varied by changing the total flow rate through the reactor tube, keeping the input reactant concentration constant. Figs. 4a and 4b are plots of $-\ln(I/I_o)$ (first order assumption) and $1/I-1/I_o$ (second order assumption) vs. reaction time [21]. I and I_o denote the mass spectral intensities of the reactant at the output and input to the reactor. The reaction temperatures were fixed at 312 and 145°C for the pyrolysis of $(C_3H_7)_3Sb$ and $(C_3H_5)_3Sb$, respectively. As seen in Fig.4a, the

relationship between $-\ln(I/I_0)$ and time is linear. That for $1/I-1/I_0$ and time is distinctly non-linear, since the data must pass through the origin [21]. The $(C_3H_7)_3Sb$ pyrolysis process is apparently first order. The $-\ln(I/I_0)$ and $1/I-1/I_0$ vs. time relationships in Fig.4b are similar. Thus, the $(C_3H_5)_3Sb$ pyrolysis process is also likely to be first order.

3.5. Effect of a Radical Scavenger

1,4-cyclohexadiene (C_6H_8) was used as a scavenger of both C_3H_7 and C_3H_5 radicals. It can effectively remove the C_3H_7 radicals yielding C_3H_8 and benzene [22]. Unfortunately, it is unknown whether C_6H_8 can completely scavenge C_3H_5 radicals. In general, C_6H_8 is believed to be more reactive than other scavengers such as benzene (C_6H_6) and toluene (C_7H_8) used to scavenge CH_3 radicals for example [23]. C_6H_8 may decompose at temperatures above 400°C producing H radicals [24] complicating the interpretation of the data in some cases. However, this does not occur at the temperatures of <350°C used in this study.

It was found that addition of 2% C_6H_8 has no effect on the pyrolysis temperature of $(C_3H_7)_3Sb$. However, the products, C_6H_{14} and C_3H_7D, disappeared in both He and D_2 ambients. This demonstrates the existence of free radicals during $(C_3H_7)_3Sb$ pyrolysis. The data clearly indicate that C_3H_7 radicals are not involved in the rate-determining reactions. They do not rapidly attack the parent molecule. Otherwise, the addition of C_6H_8 would increase the decomposition temperature.

Similarly, the addition of C_6H_8 was found to have no effect on $(C_3H_5)_3Sb$ pyrolysis. Both the decomposition temperature and the

product were unaffected in both He and D_2 ambients. These results may indicate that C_6H_8 has little effect on C_3H_5 radicals, which are considerably more stable than C_3H_7 radicals. An alternate explaination is that there are no free radicals produced during pyrolysis. Similar findings were reported for diallyltelluride ($(C_3H_5)_2Te$) pyrolysis [20]. C_6H_{10} was produced whether or not C_6H_8 was added.

3.6. Effect of the Addition of $(CH_3)_3In$

To simulate OMVPE growth, $(CH_3)_3In$ (0.03%) was mixed with $(C_3H_7)_3Sb$ and $(C_3H_5)_3Sb$ in separate experiments. Surprisingly, the $(CH_3)_3In$ signal could not be detected. Transparent liquids, presumably low volatility adduct compounds, were condensed at the In/Sb manifold area upstream from the reactor. The manifold setup in these experiments is simply a 3 inch long Y-shaped quartz tube. This makes the precursor mixing time longer than that in a real OMVPE reactor. Parasitic reactions were not observed during the growth of InSb using these precursors [7,16].

4. Discussion

4.1. $(C_3H_7)_3Sb$ Decomposition

The decomposition of $(C_3H_7)_3Sb$ is postulated to involve the following reactions:

$$(C_3H_7)_3Sb \rightarrow C_3H_7 + (C_3H_7)_2Sb \quad (1)$$
$$(C_3H_7)_2Sb \rightarrow C_3H_7 + C_3H_7Sb \quad (2)$$
$$C_3H_7Sb \rightarrow C_3H_7 + Sb \quad (3)$$
$$2C_3H_7 \rightarrow C_6H_{14} \quad (4)$$
$$2C_3H_7 \rightarrow C_3H_6 + C_3H_8. \quad (5)$$
$$C_3H_7 + D_2 \rightarrow C_3H_7D + D \quad (6)$$

$$2D \rightarrow D_2. \quad (7)$$

$$(C_3H_7)_3Sb \rightarrow C_3H_6 + (C_3H_7)_2SbH. \quad (8)$$

The rate-determining step is probably the first reaction. More radicals are released by reactions 2 and 3, resulting in Sb deposition. C_3H_7 radicals recombine and disproportionate (reactions 4 and 5) to form the products observed. For a D_2 ambient, a fraction of the radicals will react with D_2, producing C_3H_7D and D (reaction 6). No evidence of a reaction between D and $(C_3H_7)_3Sb$ was observed. The D atoms apparently recombine via reaction 7. The experimental results do not rule out reaction 8, the β-hydrogen elimination reaction. Although the trapping of C_3H_7 free radicals by C_6H_8 favors the homolysis mechanism, the observation of more C_3H_6 than C_3H_8 cannot be explained by reactions 1-7.

These pyrolysis pathways are different from those for $(CH_3)_3Sb$ pyrolysis in D_2. Although for both systems free radicals are produced and react with the D_2 ambient, D atoms are much more important for the $(CH_3)_3Sb$ pyrolysis process; the predominant product was CH_3D and the decomposition rate was enhanced in D_2 [2]. This can be understood in terms of the radical reactivity. The reactivity with D_2 is in the order of $CH_3 > C_2H_5 > C_3H_7$ [25].

4.2. $(C_3H_5)_3Sb$ Decomposition

Since the data are insufficient to uniquely define the mechanism, two schemes are discussed here.

1. Homolysis

$$(C_3H_5)_3Sb \rightarrow C_3H_5 + (C_3H_5)_2Sb. \quad (9)$$

2. Reductive Coupling

$$(C_3H_5)_3Sb \rightarrow C_6H_{10} + C_3H_5Sb. \quad (10)$$

Supplementary Reactions

$$(C_3H_5)_2Sb \rightarrow C_3H_5 + C_3H_5Sb \quad (11)$$
$$C_3H_5Sb \rightarrow C_3H_5 + Sb \quad (12)$$
$$2C_3H_5 \rightarrow C_6H_{10}. \quad (13)$$

Each scheme has something to recommend it. They are both consistent with the product (C_6H_{10}) and the homogeneous, first order nature of the overall reaction.

Homolysis has been proposed as the mechanism for pyrolysis of many group V organometallic molecules [2,17,19,26,27]. This reaction pathway, however, does not agree with the results of the free radical trapping experiment, unless C_6H_8 is unable to efficiently remove the C_3H_5 radicals from the system. Despite the fact that reductive coupling is considered to be unlikey for pyrolysis of main group organometallics [19], it has been proposed for the pyrolysis of tertiarybutylarsine ($C_4H_9AsH_2$) [28] and $(C_2H_3)_3Sb$ [17]. It has also been suggested recently for pyrolysis of $(C_3H_5)_2Te$ [20]. Being intramolecular, reductive coupling would be unaffected by a radical trap.

Since the actual rate constant for the C_3H_5/C_6H_8 reaction is unknown, it is speculative to draw any conclusions from the limited experimental data. Nevertheless, homolysis as the first step is plausible because of the extremely weak C_3H_5-Sb bond. Reductive coupling is not convincing in principle. Sb does not have an oxidation state of I and the reaction product C_3H_5Sb is not thermodynamically

stable. This kind of reaction is normally facilitated only if a lowe oxidation state is available to allow the product to have a lower potential energy, a common situation for trasition metals [19,29].

4.3. Alkyl—Sb Bond Strengths

Assuming that the homolysis step limits the pyrolysis rates for both $(C_3H_7)_3Sb$ and $(C_3H_5)_3Sb$, the alkyl-Sb bond strengths can be determined from the temperature dependence of the decomposition rate constants. The results are shown in the Arrhenius plots of Figs. 5a and 5b. The rate constant vs. temperature relationships can be expressed,

$$\log k_1\ (s^{-1}) = 11.03 - 30.8\ (\text{kcal/mole})/2.303\ RT\ (K) \quad (15)$$

$$\log k_9\ (s^{-1}) = 10.50 - 21.6\ (\text{kcal/mole})/2.303\ RT\ (K) \quad (16)$$

for $(C_3H_7)_3Sb$ and $(C_3H_5)_3Sb$, respectively. The activation energies indicate bond strengths which are signifiantly lower than those for CH_3—Sb (62.3 kcal/mole) and C_2H_3—Sb (49.0 kcal/mole) [2,17].

4.4. Possibility of Adduct Formation

The use of low alkyl-metal bond-strength precursors for low temperature OMVPE has some potentially negative consequences. For example, the probability of forming adducts with the group III precursors, leading to unwanted parasitic reactions, may be increased. The stability of the Lewis acid/base adduct can be determined by estimating the strengths of the acid and base. The basicity of the group V precursors is reflected by the stability of the carbonium ion of the ligand groups. The more stable the carbonium ion, the more basic the precursor will be: As more electron density is shifted to the lone pair of the group V element, the precursor will be

more electron-donating. For example, stability of the carbonium ions is in the order $CH_3^+ < C_2H_5^+ < C_4H_9^+$ [25]. The probability of the precursor forming an adduct with trimethylgallium ($(CH_3)_3Ga$) increases as the group V precursor changes from trimethylarsine ($(CH_3)_3As$) to $(C_2H_5)_3As$ to tritertiarybutylarsine ($(C_4H_9)_3As$). This adduct formation trend, also applicable to $(CH_3)_3In$ with Sb precursors, has been experimentally observed (assuming that the observed liquids represent the adducts) [30]. On the other hand, comparing the tri-, di-, and mono-alkyl precursors, the probability of forming an adduct (the liquid) with $(CH_3)_3Ga$ is in the order $(C_2H_5)_3As$ >diethylarsine ($(C_2H_5)_2AsH$) >monoethylarsine ($C_2H_5AsH_2$) [31]. This is because the alkyl ligand delocalizes electrons more effectively than the H ligand [25]. Precursors with more alkyl ligands have higher lone pair electron densities. This makes these precursors more electron-donating and more likely to form an adduct.

Both $C_3H_7^+$ and $C_3H_5^+$ are stable carbonium ions, considering the low C_3H_7—H and C_3H_5—H bond strengths [25]. Thus, it is not surprising that the tri-alkyls $(C_3H_7)_3Sb$ and $(C_3H_5)_3Sb$ will likely form adducts with $(CH_3)_3In$.

4.5. Use for OMVPE Growth

The lower pyrolysis temperatures for $(C_3H_7)_3Sb$ and $(C_3H_5)_3Sb$, as compared to those for $(CH_3)_3Sb$ and $(C_2H_3)_3Sb$, suggest that they are more suitable for low temperature OMVPE growth of Sb-containing materials. However, due to the possibility of adduct formation with the group III precursor, the reactor should be carefully designed to avoid parasitic reactions.

5. Summary

The pyrolysis reactions for $(C_3H_7)_3Sb$ and $(C_3H_5)_3Sb$ have been investigated in He and D_2 ambients. $(C_3H_7)_3Sb$ and $(C_3H_5)_3Sb$ pyrolyze in the temperature ranges from 250 to 350°C and from 100 to 160°C, respectively. The ambient has no effect on the decomposition temperature of either precursor. For $(C_3H_7)_3Sb$, a deuterated product, C_3H_7D, was produced in D_2 in addition to the C_3H_6, C_3H_8, and C_6H_{14} (2,3-dimethylbutane) produced in He. For $(C_3H_5)_3Sb$, the only major product is C_6H_{10} (1,5-hexadiene) in both He and D_2. The pyrolysis reactions for both precursors are homogeneous and first order. The addition of a radical scavenger C_6H_8 inhibited the formation of C_3H_7D and C_6H_{14} in $(C_3H_7)_3Sb$ pyrolysis, but the C_6H_{10} is still produced in $(C_3H_5)_3Sb$ pyrolysis. The $(C_3H_7)_3Sb$ decomposition probably begins via cleavage of the Sb-C bonds. However, for $(C_3H_5)_3Sb$ pyrolysis two possibilities, homolysis and reductive coupling, were proposed. Assuming that homolysis is the rate-determining step for both $(C_3H_7)_3Sb$ and $(C_3H_5)_3Sb$, bond strengths of 30.8 and 21.6 kcal/mole for C_3H_7—Sb and C_3H_5—Sb, respectively, were suggested. When $(CH_3)_3In$ was present, liquids, presumably adducts, between the In and Sb precursors were observed.

6. Acknowledgement

This work was sponsored by the Air Force Office of Scientific Research, the Office of Naval Research, and the Office of Naval Technology.

7. References

1. G. B. Stringfellow, *OMVPE, Theory and Practice*, (Academic Press, Boston, 1989)
2. C. A. Larsen, S. H. Li, and G. B. Stringfellow, Chemistry of Materials, to be published.
3. K. Y. Ma, Z. M. Fang, D. H. Jaw, R. M. Cohen, G. B. Stringfellow, W. P. Kosar, and D. W. Brown, Appl. Phys. Lett. **55**, 2420 (1989)
4. R. M. Biefeld, J. Crystal Growth, **75**, 255 (1986)
5. K. Y. Ma and G. B. Stringfellow, unpublished results.
6. G. T. Stauf, D. K. Gaskill, N. Bottka, and R. W. Gedridge, Paper T5.6, MRS Meeting, Boston, Massachusetts, November, 1990.
7. C. H. Chen, G. B. Stringfellow, and R. W. Gedridge, Jr., OMVPE Work Shop, Panama City Beach, Florida, 1991.
8. T. H. Lowry and K. S. Richardson, *Mechanism and Theory in Organic Chemistry*, (3rd edition, Harper & Row, N. Y., 1987) p.747, chapter 9
9. N. I. Buchan, C. A. Larsen and G. B. Stringfellow, Appl. Phys. Lett., **51**, 1024 (1987)
10. D. F. Shriver and M. A. Dredzon, *The Manipulations of Air-Sensitive Compounds*, (2nd ed., John Wiley & Sons, N. Y., 1986)
11. H. J. Breunig and W. Kanig, J. Organometallic Chem., **C5**, 186 (1980)
12. A. E. Borisov, N. V. Novikova, and A. N. Nesmeyanov, Izvest. Akad. Nauk SSSR, Ser. Khim., 1506 (1963); Chem. Abst. 59, 14021
13. F. W. McLafferty and D. B. Stauffer, *The Wiley/NBS Registry of Mass Spectral Data*, (Vol.1, John Wiley & Sons, N. Y., 1989)

14. J. W. Otvos and D. P. Stevenson, J. Am. Chem. Soc., **78**, 546 (1956)

15. Data from CVD Metalorganics; L. Maier, D. Seyferth, F. G. A. Stone, and E. G. Rochow, J. Amer. Chem. Soc., **79**, 5884 (1957)

16. C. H. Chen, private communication.

17. C. A. Larsen, R. W. Gedridge, Jr., and G. B. Stringfellow, Chemistry of Materials, to be published; C. A. Larsen, R. W. Gedridge, Jr., S. H. Li, and G. B. Stringfellow, Paper E5.29, MRS Meeting, Boston, Massachusetts, November, 1990.

18. S. H. Li, unpublished data; chapter 4 of Ref.1.

19. P. W. Lee, T. R. Omstead, D. R. McKenna, and K. F. Jensen, J. Crystal Growth, **93**, 134 (1988)

20. R. U. Kirss, D. W. Brown, K. T. Higa, and R. W. Gedridge, Jr., Organometallics, to be published.

21. O. Levenspiel, *Chemical Reaction Engineering*, 2nd. Edition, (John Wiley & Sons, Inc., N. Y., 1972) Chapter 2

22. V. N. Konddratiev, *Rate Constants of Gas Phase Reactions*, (National Bureau of Standards, U. S. Depart. of Commerce, Washington, D. C., 1972) p.171

23. J. A. Kerr and M. J. Parsonage, Evaluated Kinetic Data on Gas Phase Hydrogen Transfer Reactions of Methyl Radicals, (Butterworths, London, 1976) p.76, p79, and p.80,

24. C. A. Larsen, S. H. Li, N. I. Buchan, and G. B. Stringfellow, J. Crystal Growth, **102**, 126 (1990)

25. T. W. G. Solomons, *Organic Chemistry*, (John Wiley & Sons, Inc., N.Y., 1976) p.123, p.174

26. S. H. Li, C. A. Larsen, and G. B. Stringfellow, J. Crystal Growth, **102**, 117 (1990)

27. S. H. Li, C. A. Larsen, and G. B. Stringfellow, J. Crystal Growth, to be published.

28. C. A. Larsen, N. I. Buchan, S. H. Li, and G. B. Stringfellow, J. Crystal Growth, **93**, 15 (1988)

29. G. Wilkinson, F. G. Stone, and E. W. Abel, *Comprehensive Organometallic Chemistry*, (Pergamon, Oxford, 1982) Chapter 19

30. S. H. Li, unpublished data; $(C_4H_9)_3As$ has not been combined with TMGa, however, the combination of $(C_4H_9)_2AsH$ and $(CH_3)_3Ga$ led to a stable liquid material. The combination of $(C_2H_5)_3As$+$(CH_3)_3Ga$ also led to a liquid material. But, the combination of $(CH_3)_3As$+$(CH_3)_3Ga$ did not.

31. S. H. Li, C. A. Larsen, and G. B. Stringfellow, J. Electronic Materials, to be published.

Captions

Fig.1 Temperature dependence of percent decomposition for several Sb precursors: $(C_3H_7)_3Sb$ (TiPSb, 0.05%), $(C_3H_5)_3Sb$ (TASb, 0.05%), $(CH_3)_3Sb$ (TMSb, 1%), and $(C_2H_3)_3Sb$ (TVSb, 1%). (■) in He; (□) in D_2; (◇) in D_2 with a high surface area.

Fig.2 Pyrolysis products of 0.05% $(C_3H_7)_3Sb$ in (a) He and (b) D_2.

Fig.3 Pyrolysis products of 0.05% $(C_3H_5)_3Sb$ in (a) He and (b) D_2.

Fig.4 $-\ln(I/I_o)$ and $1/I-1/I_o$ vs. reaction time: (a) $(C_3H_7)_3Sb$ in D_2, 312°C; (b) $(C_3H_5)_3Sb$ in D_2, 145°C.

Fig.5 Temperature dependences of the pyrolysis rate constants for (a) $(C_3H_7)_3Sb$ and (b) $(C_3H_5)_3Sb$.

Table 1. Vapor Pressures of $(C_3H_7)_3Sb$ and $(C_3H_5)_3Sb$

$(C_3H_7)_3Sb$		$(C_3H_5)_3Sb$	
Temp.(°C)	V. P. (Torr)	Temp.(°C)	V. P. (Torr)
30-31	0.7	31-32	0.35
32-33	0.8	34-35	0.5
34	0.6	45-46	1.0
44	1.6	56	1.35
53-54	2.5	61	1.5
57-58	3.25	71	2.0 (Ref.12)
59-60	4.0		
logP(Torr)=9.268-2881/T(K)		logP(Torr)=6.089-1973/T(K)	

Table 2. Major Mass Spectral Peaks (70 eV) for $(C_3H_7)_3Sb$ and $(C_3H_5)_3Sb$

$(C_3H_7)_3Sb$		$(C_3H_5)_3Sb$	
m/e	Rel. %	m/e	Rel. %
43	100	41	100
165	61	39	68
41	47	67	56
167	36	163	56
251	22	82	50
39	22	204	44
45	22	137	14

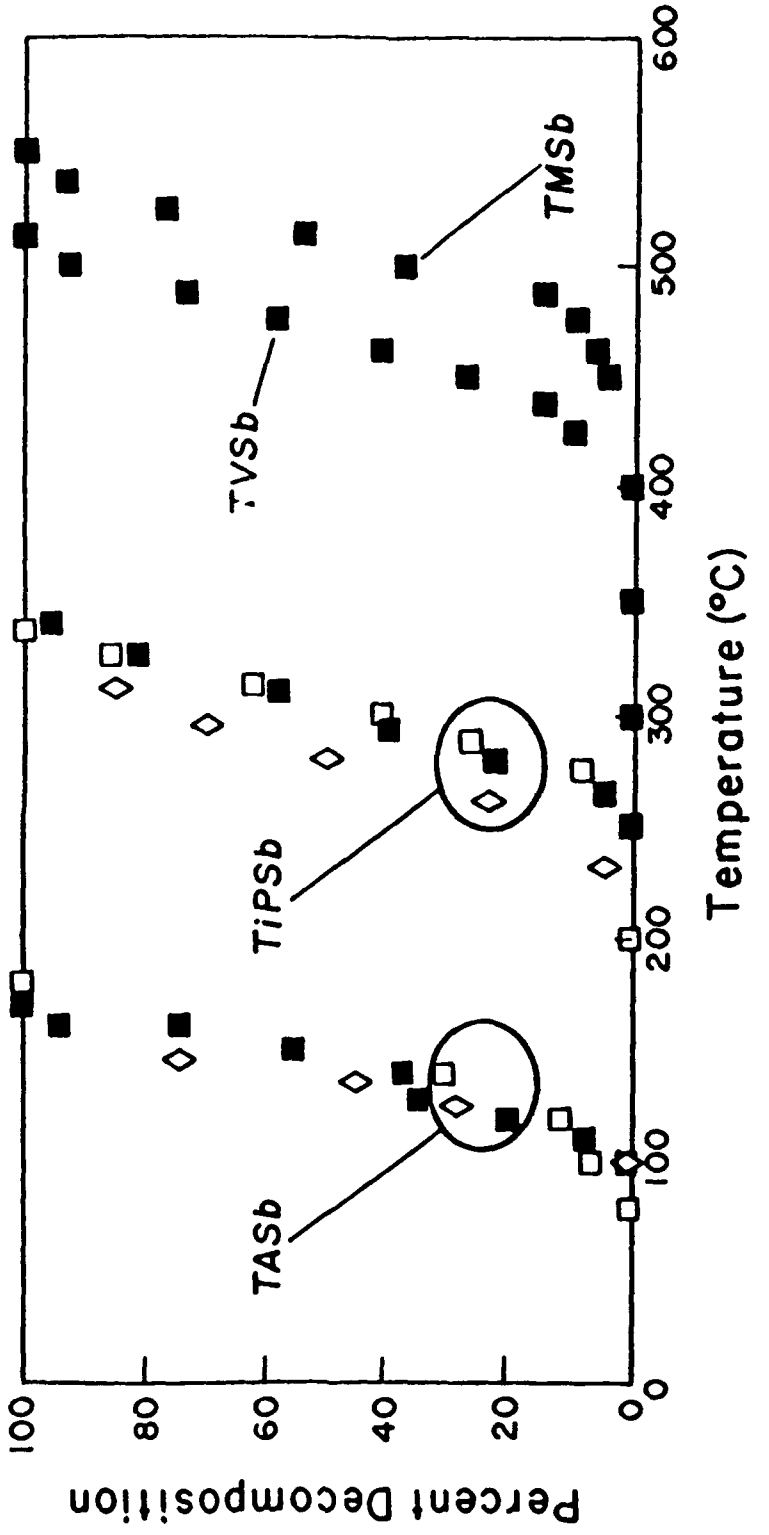
Percent Decomposition
0
20
40
60
80
100
Temperature (°C)
0
100
200
300
400
500
600
TMSb
TVSb
TiPSb
TASb

Fig. 1

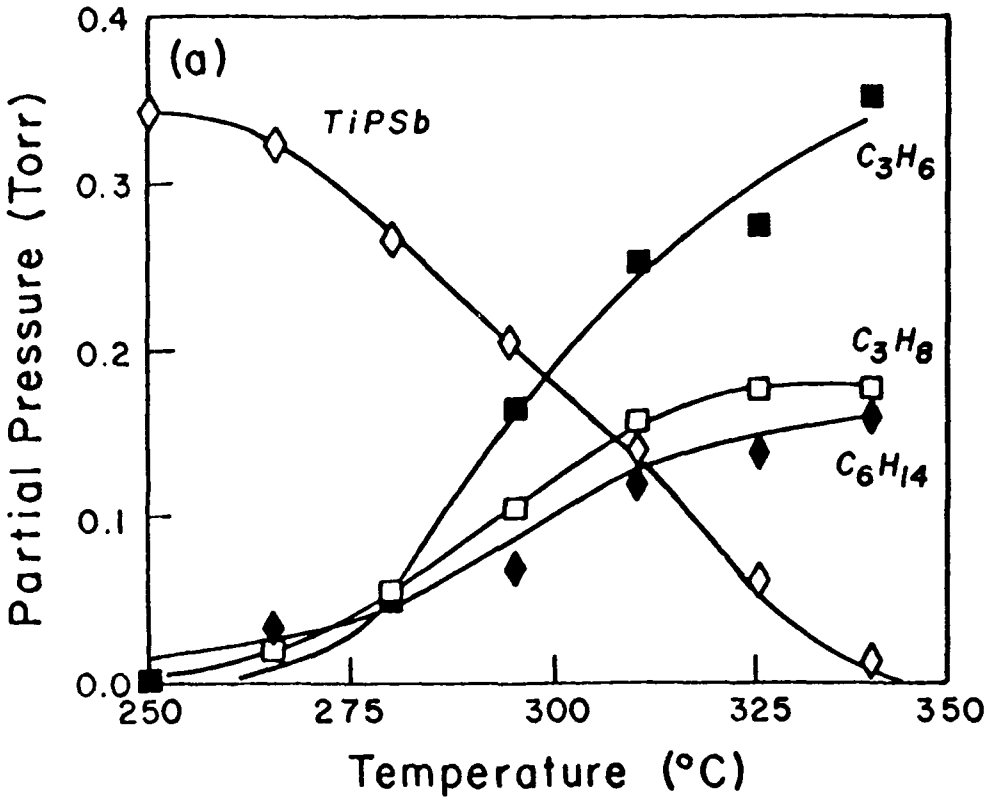
(a)
TiPSb
C_3H_6
C_3H_8
C_6H_{14}
Partial Pressure (Torr)
0.0
0.1
0.2
0.3
0.4
250
275
300
325
350
Temperature (°C)

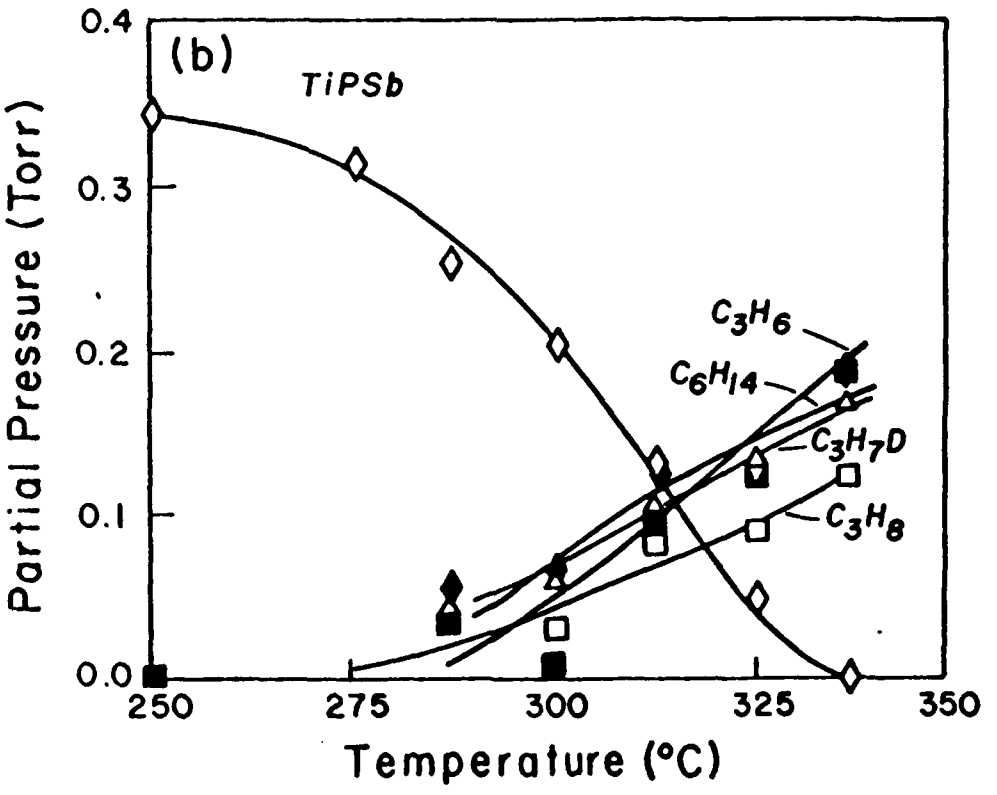
(b)
TiPSb
C_3H_6
C_6H_{14}
C_3H_7D
C_3H_8
Partial Pressure (Torr)
0.0
0.1
0.2
0.3
0.4
250
275
300
325
350
Temperature (°C)

Fig 2

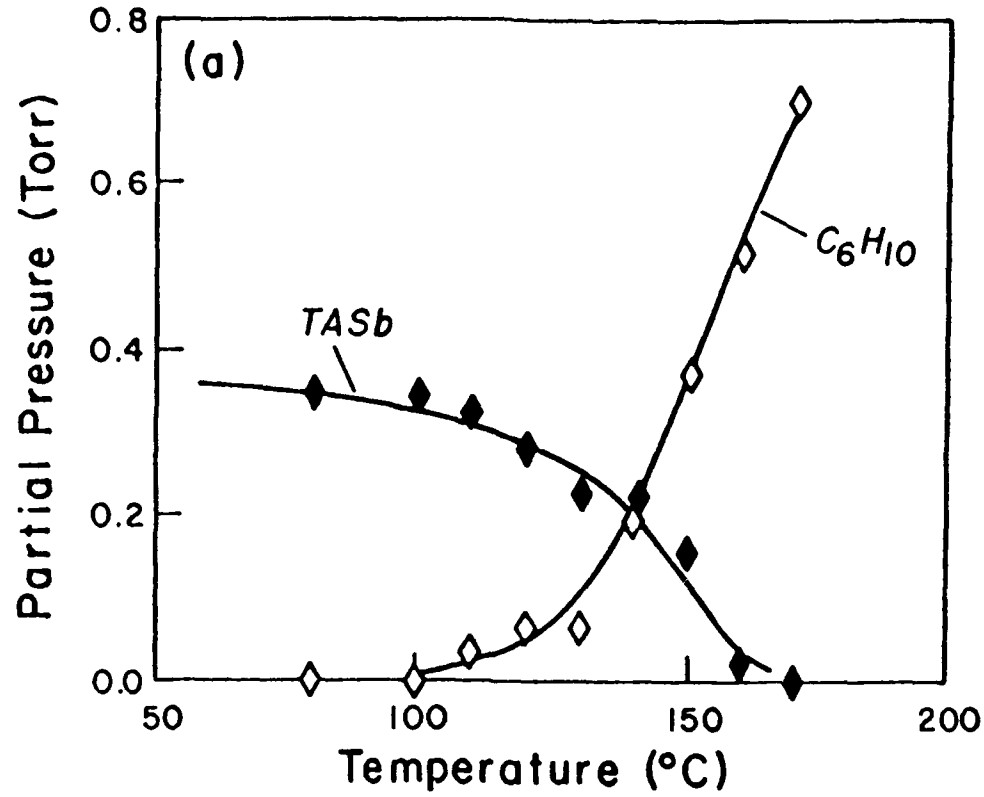
(a)
Partial Pressure (Torr)
0.8
0.6
0.4
0.2
0.0
TASb
C_6H_{10}
50
100
150
200
Temperature (°C)

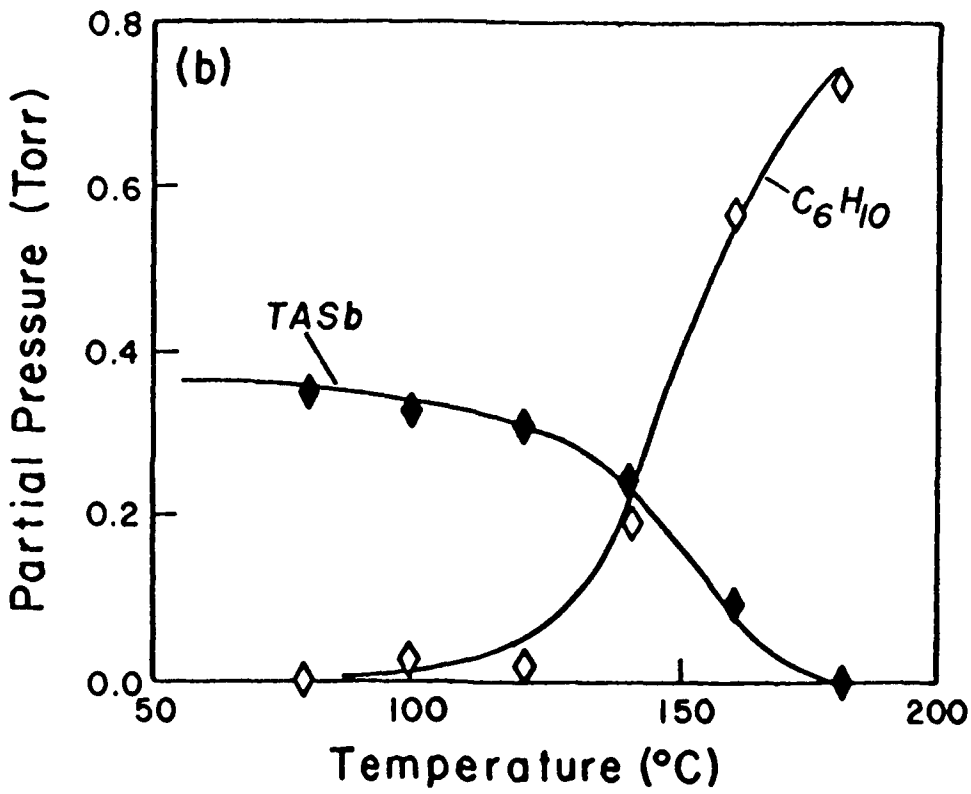
(b)
Partial Pressure (Torr)
0.8
0.6
0.4
0.2
0.0
TASb
C_6H_{10}
50
100
150
200
Temperature (°C)

Fig 3

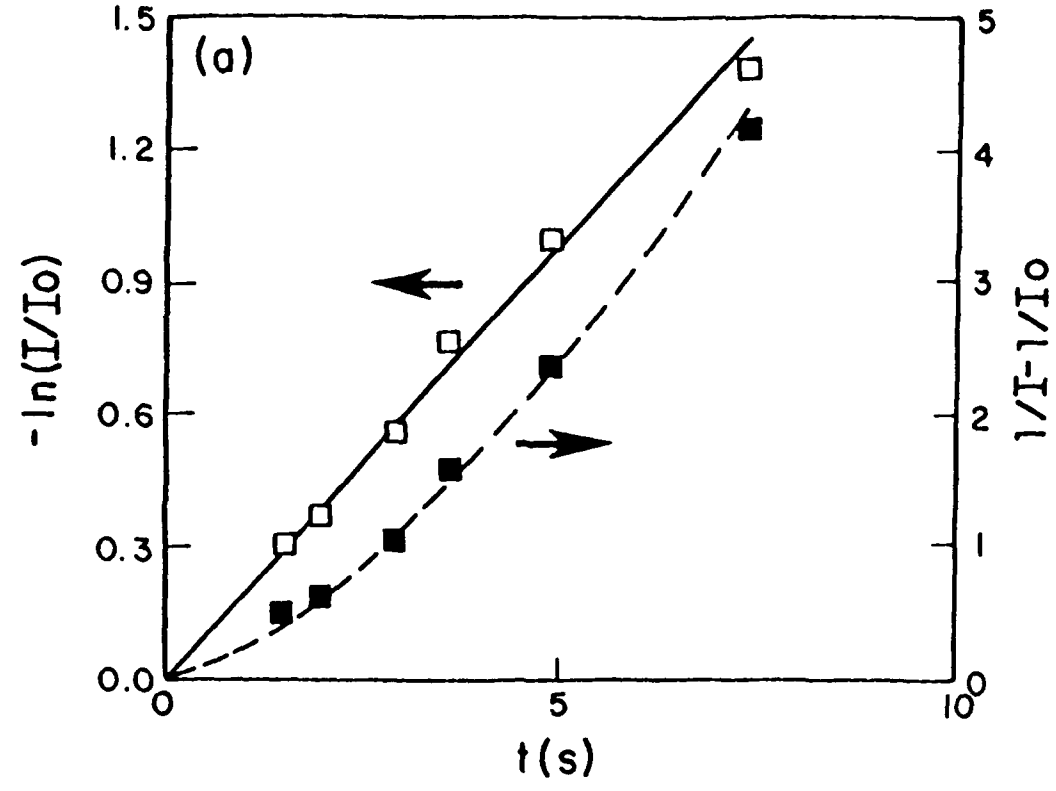
(a)
1.5
1.2
0.9
0.6
0.3
0.0
-ln(I/Io)
0
5
10
t(s)
5
4
3
2
1
0
1/I-1/Io

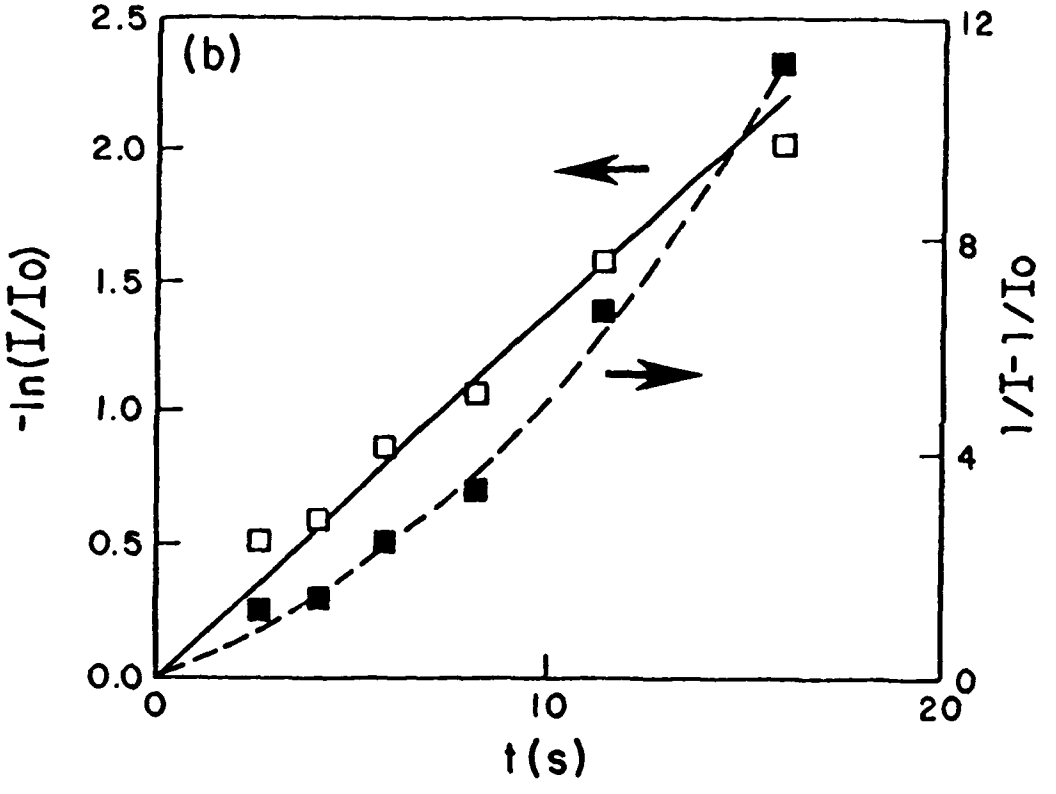
(b)
2.5
2.0
1.5
1.0
0.5
0.0
-ln(I/Io)
0
10
20
t(s)
12
8
4
0
1/I-1/Io

Fig 4

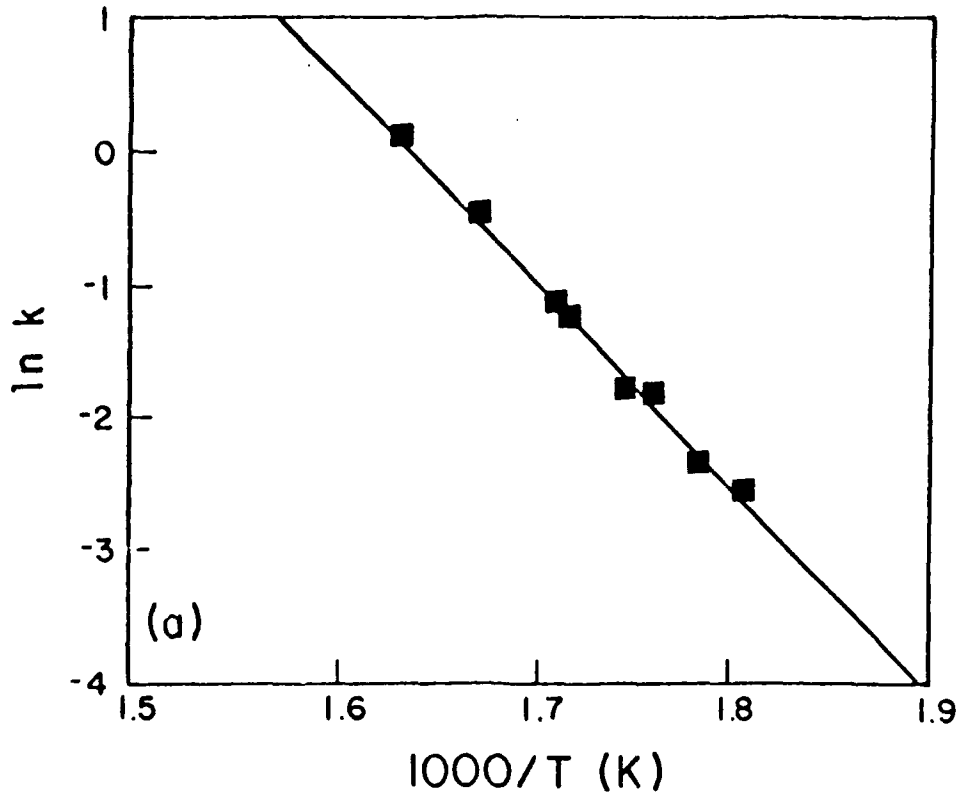
1
0
-1
-2
-3
-4
ln k
(a)
1.5
1.6
1.7
1.8
1.9
1000/T (K)

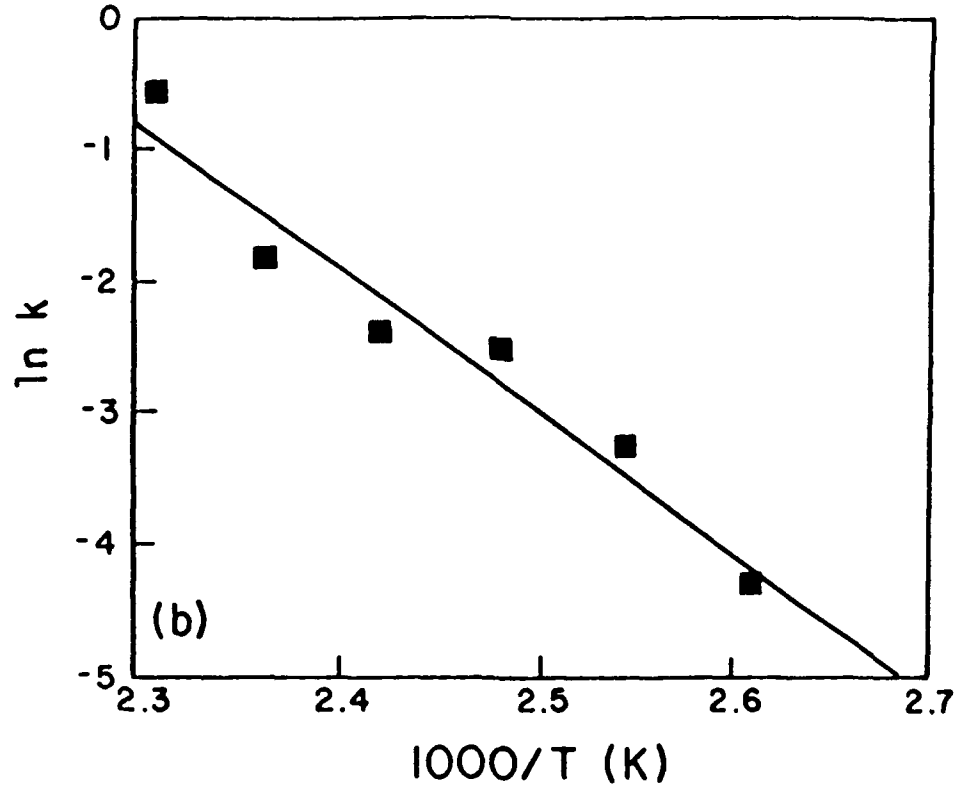
0
-1
-2
-3
-4
-5
ln k
(b)
2.3
2.4
2.5
2.6
2.7
1000/T (K)

Fig 5